JOURNAL OF AIRCRAFT
Vol. 32, No. 5, September–October 1995

Analytic Sensitivity and Approximation of Skin Buckling Constraints in Wing-Shape Synthesis

Eli Livne* and Radomir Milosavljevic†
University of Washington, Seattle, Washington 98195

Explicit expressions for terms of the stiffness and geometric stiffness matrices are derived for the buckling analysis of trapezoidal fiber composite wing skin panels. The formulation is based on Ritz analysis using simple polynomials, and leads to explicit expressions for the analytic sensitivities of the stiffness and geometric stiffness matrices with respect to layer thickness, fiber directions, and panel shape. Integration with wing box analysis using either the equivalent plate approach or the finite element method, makes it possible to obtain sensitivities of panel buckling constraints with respect to wing planform shape or locations of internal ribs and spars. The analytic sensitivities are used to construct approximations of panel buckling constraints for integrated wing/panel design synthesis.

Nomenclature

$[A]$	= in-plane local stiffness matrix for the plate, 3×3
$[D]$	= out-of-plane local stiffness matrix for the plate, 3×3
$F_B(x, y)$	= weight function ensuring zero displacement on panel boundary
F_{ij}^{qp}	= coefficients in the polynomial expression for $[F_3]$, Eq. (30)
$[F_1]$, $[F_2]$, $[F_3]$	= matrices containing admissible functions and their derivatives, Eqs. (2–4)
$f_i(x, y)$	= admissible functions
$\overline{H_{ih}}$	= coefficients of wing depth polynomial
$\overline{H(x, y)}$	= depth of wing
h	= total thickness of panel
I_{TR}	= integral of a simple polynomial term over trapezoidal panel area
i, i_1, i_2	= indices of terms in layer thickness polynomials
$[K]$, $[K_G]$	= stiffness and geometric stiffness matrix, respectively
M_x, M_y, M_{xy}	= internal moments per unit length
$mf2_{ij}^{qp}$, $nf2_{ij}^{qp}$	= powers of x and y in elements of $[F_2]$, Eq. (51)
m, n	= powers of x and y in a polynomial term
m_h, n_h	= powers of x and y in the wing depth series
$\bar{m}_{qw,pw}$, $\bar{n}_{qw,pw}$	= powers of x and y for elements of α
m_j^u, n_j^u, n_j^u	= powers of x and y in polynomial terms of $[F_3]$, Eq. (15)
m_k^{ti}, n_k^{ti}	= powers of x and y in polynomial series for thickness of layer i
m_p^w, n_p^w	= powers of x and y in Ritz functions, Eq. (17)
$[N]$	= 2×2 matrix of in-plane loads, Eq. (5)
N_i	= number of terms in the thickness polynomial for layer i
N_L	= number of layers
N_x, N_y, N_{xy}	= in-plane loads per unit length
$[\bar{\bar{Q}}]$	= 3×3 constitutive matrix for a layer, Eq. (22)
$[Q_i]$	= material properties matrix, Eqs. (20) and (21)
q_p, $\{q\}$	= generalized displacement and the vector of generalized displacements for panel
R, S	= coefficients of front line or aft line of panel
T_j^i	= coefficient j in the polynomial series for layer i
$t_i(x, y)$	= thickness of layer i
U_i, V_j	= shape dependent coefficients of F_B, Eqs. (15) and (16)
$W_{qw,pw}$	= coefficients of polynomial elements of α
$w^1(x, y)$	= panel elastic out-of-plane displacement
$[\alpha]$	= matrix of function derivatives defined in Eq. (41)
θ	= fiber orientation angle
λ	= buckling eigenvalue

Subscripts

A	= aft (rear)
F	= front
L	= left
R	= right

Introduction

BUCKLING of skin panels in thin-walled structures is one of the most important failure modes to be considered in any design synthesis. A rich body of literature exists today on the buckling of isotropic and anisotropic panels.[1–5] It reflects the extensive experience in this area, based on theoretical development, numerical investigations, and numerous tests.

While the study of isolated panels of rectangular shape has reached certain maturity, research addressing the buckling of panels functioning as components in a larger structural system is still evolving. In the complete structure, such as an airplane wing or fuselage, buckling can occur locally (when a particular panel buckles) or globally (when a segment of the structure, containing several panels, buckles). The need to assess global behavior (for internal force distributions or global buckling) and local behavior (panel buckling) simultaneously, leads to computationally intensive analysis. The complex global–local interactions can also make buckling constraints highly nonlinear in terms of the structural design variables. Thus, in the context of airframe structural optimization, proper represen-

Received Aug. 30, 1994; revision received March 24, 1995; accepted for publication March 31, 1995.

*Assistant Professor, Department of Aeronautics and Astronautics. Senior Member AIAA.

†Graduate Student, Department of Aeronautics and Astronautics.

tation of buckling constraints is a major challenge, and it is still an area of active research.[6-15]

When wing planform becomes subject to design optimization in addition to the sizing of structural members, or when variation of the internal structure is allowed, the panel buckling problem becomes more complex. In the more general case, panels (as defined by the array of ribs and spars that supports them) are rarely rectangular. They are usually trapezoidal in shape. Moreover, while in high AR wings it may be acceptable to assume unidirectional compression on the skin panels, in low AR wings panels are usually loaded by inplane loads in an inherently combined manner.

It is important, then, to develop an efficient buckling analysis methodology, applicable to trapezoidal panels in combined in-plane loading.[16-18] Such a methodology should be design-oriented, i.e., issues of sensitivity analysis and approximation concepts should be addressed from the outset. Integration of the wing box global analysis with the local panel buckling analysis should be fast computationally. The result should be an efficient structural analysis, sensitivity, and approximation tool for wing shape optimization, including stress, deformation, dynamic behavior, and panel buckling constraints.

In this article, a method for buckling analysis of trapezoidal wing composite skin panels is presented. Analytic sensitivities of buckling constraints with respect to sizing, fiber directions, and panel shape are derived. Integration of the resulting buckling analysis with an approximate wing box structural analysis based on the equivalent plate approach[19-21] or finite element analysis is discussed. Alternative approximation techniques are assessed. Lessons learned and the resulting recommendations will help guide further developments on the way to effective wing shape optimization in the preliminary design stage.

This article opens by deriving the general equations for panel buckling analysis for simply supported trapezoidal panels. The Ritz method, using polynomial admissible functions, is employed. Detailed derivations, taking advantage of the simplicity of manipulation of polynomials, demonstrate how stiffness and geometric stiffness terms can be expressed in terms of sizing, fiber direction, and shape design variables explicitly. The integration of wing box structural analysis with panel buckling analysis is discussed next, followed by a method for the computation of analytic sensitivities. Results of numerical evaluations and lessons learned conclude the presentation.

Ritz Panel Buckling Analysis and Constraint Formulation

Stability Equations

Based on the principle of virtual work, a variational equation for a symmetrically layered composite plate under the action of internal bending moments and transverse shear forces in the absence of transverse load or initial deformation is

$$\iint \{w^1_{,xx} \quad w^1_{,yy} \quad 2w^1_{,xy}\}[D]\delta \begin{Bmatrix} w^1_{,xx} \\ w^1_{,yy} \\ 2w^1_{,xy} \end{Bmatrix} \mathrm{d}x\,\mathrm{d}y + \iint \{w^1_{,x} \quad w^1_{,y}\} \begin{bmatrix} N_x & N_{xy} \\ N_{xy} & N_y \end{bmatrix} \delta \begin{Bmatrix} w^1_{,x} \\ w^1_{,y} \end{Bmatrix} \mathrm{d}x\,\mathrm{d}y = 0 \tag{1}$$

where the vertical deflection due to load is $w^1(x, y)$. The matrices $[D]$ (and a corresponding matrix $[A]$) are the 3×3 local transverse stiffness (and in-plane stiffness) matrices, respectively.[1,2] In the case of a symmetrically layered panel, the in-plane loads N_x, N_y, and N_{xy} are related to the in-plane strains $\{\varepsilon^0_x \; \varepsilon^0_y \; \gamma^0_{xy}\}$ through the matrix $[A]$. The bending moments M_x, M_y, and M_{xy} are related to the bending curvatures due to load $\{-w^1_{,xx} \; -w^1_{,yy} \; -2w^1_{,xy}\}$ through the matrix $[D]$ (Refs. 1 and 2).

The unknown elastic panel deflection $w^1_{(x,y)}$ is approximated by a series of admissible functions:

$$w^1_{(x,y)} = \sum_{p=1}^{N} f_{p(x,y)} q_p = \{f_{1(x,y)} \quad f_{2(x,y)} \quad \cdots \quad f_{N(x,y)}\} \begin{Bmatrix} q_1 \\ q_2 \\ \cdot \\ q_N \end{Bmatrix} = [F_1]\{q\} \tag{2}$$

The first derivatives, then, can be expressed as

$$\begin{Bmatrix} w^1_{,x} \\ w^1_{,y} \end{Bmatrix} = \begin{bmatrix} f_{1,x} & f_{2,x} & \cdots & f_{N,x} \\ f_{1,y} & f_{2,y} & \cdots & f_{N,y} \end{bmatrix} \begin{Bmatrix} q_1 \\ q_2 \\ \cdot \\ q_N \end{Bmatrix} = [F_2]\{q\} \tag{3}$$

and the second derivatives are given by

$$\begin{Bmatrix} w^1_{,xx} \\ w^1_{,yy} \\ 2w^1_{,xy} \end{Bmatrix} = \begin{bmatrix} f_{1,xx} & f_{2,xx} & \cdots & f_{N,xx} \\ f_{1,yy} & f_{2,yy} & \cdots & f_{N,yy} \\ 2f_{1,xy} & 2f_{2,xy} & \cdots & 2f_{N,xy} \end{bmatrix} \begin{Bmatrix} q_1 \\ q_2 \\ \cdot \\ q_N \end{Bmatrix} = [F_3]\{q\} \tag{4}$$

In the previous expressions the matrices $[F_1]$, $[F_2]$, and $[F_3]$ are all functions of x and y. Using Eqs. (2–4) to express virtual displacements and their derivatives in terms of virtual generalized displacements, $\delta w^1 = [F_1]\{\delta q\}$, Eq. (1) leads to

$$\{q\}^T \iint [F_3]^T[D][F_3]\,\mathrm{d}x\,\mathrm{d}y\,\{\delta q\} + \{q\}^T \iint [F_2]^T[N][F_2]\,\mathrm{d}x\,\mathrm{d}y\,\{\delta q\} = 0 \tag{5}$$

where

$$[N] = \begin{bmatrix} N_x & N_{xy} \\ N_{xy} & N_y \end{bmatrix}$$

The matrix equation for the linear buckling analysis of the panel is thus

$$[[K] + \lambda[K_G]]\{q\} = \{0\} \tag{6}$$

where the stiffness matrix is

$$[K]_{N\times N} = \iint [F_3]^T[D][F_3]\,\mathrm{d}x\,\mathrm{d}y \tag{7}$$

and the geometric stiffness matrix is

$$[K_G]_{N\times N} = \iint [F_2]^T[N][F_2]\,\mathrm{d}x\,\mathrm{d}y \tag{8}$$

The scalar λ is used as a scaling parameter increasing or decreasing the given in-plane loads N_{ij} simultaneously, to determine whether the panel is stable or unstable. Equation (6) is a generalized linear eigenvalue problem. Since the stiffness and geometric stiffness matrices are real and symmetric, the eigenvalues are real. The buckling constraint for the panel is in the form

$$1 - \lambda_{\min} \leq 0 \tag{9}$$

assuring that the given in-plane loads have to be increased to reach instability.

Simple Polynomials for Modeling and Approximation

Admissible functions based on simple polynomials, as is well known,[28] lead to ill-conditioned system matrices. As the order of the approximation polynomials is increased, high-order terms and low-order terms appear simultaneously in the stiffness and geometric stiffness matrices. Large differences in order of magnitude among those terms will lead to ill-conditioned linear equation and eigenvalue solutions on a finite word-length computer. Unless convergence of the solution is obtained with low-order polynomials, it may become impossible to achieve convergence at all, if the order of polynomial functions is increased to the point where the equations become ill conditioned.

Still, simple polynomials offer significant advantages in structural analysis, especially in the case of beam- and plate-like structures. Simple polynomials are easily manipulated, and therefore, the formulation of the problem for solution becomes quite simple. They can also lead to integrals that may be evaluated analytically. Numerical quadrature is not required, and the solution process becomes significantly faster. Simple polynomials have been used as admissible functions in plate vibration problems[29,30] and in shells.[31] In the context of wing optimization, simple polynomials were found to lead to acceptable deformation, stress, and mode shapes in wings of quite complex planforms.[21-27] The resulting structural analysis capabilities were found to be very efficient computationally.

When planform shape variations are allowed (in addition to sizing changes, during wing optimization), using simple polynomials for structural analysis makes it possible to obtain structural shape sensitivities analytically. As Ref. 25 shows, it is possible to obtain closed-form expressions for the shape derivatives of wing box stiffness and mass terms avoiding numerical quadrature. In wing design-oriented structural analysis involving shape design variables, there is a need to evaluate buckling constraints for panels whose shape is changing. Buckling constraint sensitivities with respect to the shape of a panel, linked to variations in the shape of the wing, are also required. Based on existing experience with wing box modeling and shape sensitivity analysis, simple polynomials (multiplied by appropriate weight polynomial functions) are used in the present work for the panel buckling analysis. The simplicity of formulation, computational efficiency, and ease with which analytical shape sensitivities are obtained provide the motivation. Convergence studies show fast convergence with a small number of polynomial terms and no ill-conditioning problems. Straightforward integration of local level panel and global level wing box solutions is an additional advantage.

Modeling

In the polynomial-based wing box analysis, the thickness of fibers in different directions is given by simple polynomials. For layer i (out of N_L layers)

$$t_{i(x,y)} = T_1^i + T_2^i x + T_3^i y + T_4^i x^2 + \cdots = \sum_{k=1}^{N_i} T_k^i \cdot x^{(m_k^i)} \cdot y^{(n_k^i)}, \qquad i = 1, N_L \tag{10}$$

The powers m_k^i and n_k^i are x and y powers of the kth term of the thickness series for the ith layer. The coefficients T_k^i serve as sizing-type design variables. Unlike many studies, in which wing trapezoidal segments are transformed into a unit square for numerical quadrature, here the thickness polynomial is given in terms of the physical x, y coordinates (Fig. 1). The overall thickness of skin panels is given by Eq. (10)

$$h_{(x,y)} = \sum_{i=1}^{N_L} t_{i(x,y)} = \sum_{i=1}^{N_L} \sum_{k=1}^{N_i} T_k^i \cdot x^{(m_k^{t_i})} \cdot y^{(n_k^{t_i})} \tag{11}$$

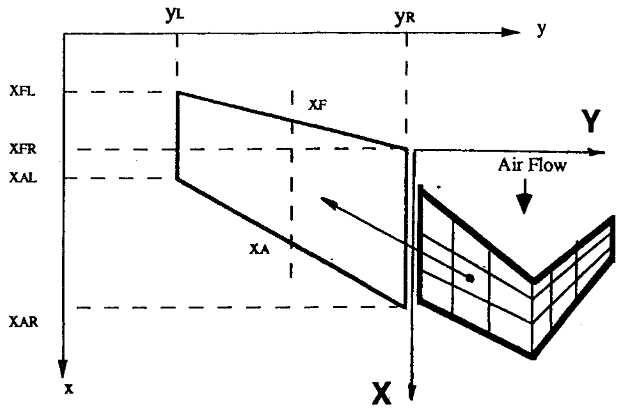

Fig. 1 Wing planform, internal structure, and skin panels geometry: panel shape design variables.

In a similar manner, cap areas for the spars and ribs of the wing box model are also expressed as simple polynomials of either x (for ribs) or y (for spars).[21-23,25-27] Depth of the wing box is also given by a simple polynomial in x and y, to be defined later.

Admissible Functions

Figure 1 shows a trapezoidal panel defined by coordinates of its vertices in the x, y axes. The subscripts L and R denote left and right sides, respectively. The subscripts F and A denote front and aft lines, respectively, and x_F and x_A are the x coordinates of the forward and rear points on a line parallel to the sides of the panel. Based on Fig. 1, we can write the following equation for points on the front line:

$$x_F(y) = \left(\frac{x_{FL} y_R - x_{FR} y_L}{y_R - y_L}\right) + \left(\frac{x_{FR} - x_{FL}}{y_R - y_L}\right) y = R_F + S_F y \tag{12}$$

In a similar way, on the rear line, expressing x_A in terms of y leads to

$$x_A(y) = \left(\frac{x_{AL} y_R - x_{AR} y_L}{y_R - y_L}\right) + \left(\frac{x_{AR} - x_{AL}}{y_R - y_L}\right) y = R_A + S_A y \tag{13}$$

The function $F_B(x, y) = [x - S_F y - R_F][x - S_A y - R_A][y - y_L][y - y_R]$ satisfies the zero displacement boundary conditions on the circumference of the panel. Using Eqs. (12) and (13), and expanding in terms of x and y yields

$$F_{B(x,y)} = (U_1 + U_2 y + U_3 y^2) \times \{V_1 + V_2 x + V_3 y + V_4 x^2 + V_5 xy + V_6 y^2\} \tag{14}$$

and, using index notation

$$F_{B(x,y)} = \sum_{i=1}^{3} U_i y^{n_i^u} \sum_{j=1}^{6} V_j x^{m_j^v} y^{n_j^v} = \sum_{i=1}^{3} \sum_{j=1}^{6} U_i V_j x^{m_j^v} y^{n_i^u + n_j^v} \tag{15}$$

where the constants U and V are given in terms of panel vertex coordinates by

$$\begin{gathered} U_1 = y_L y_R, \quad U_2 = -(y_L + y_R), \quad U_3 = 1, \quad V_1 = R_A R_F \\ V_2 = -(R_A + R_F), \quad V_3 = (R_A S_F + R_F S_A) \\ V_4 = 1, \quad V_5 = -(S_A + S_F), \quad V_6 = S_F S_A \end{gathered} \tag{16}$$

Powers of x and y corresponding to constants U and V [Eq. (15)] are given in Tables 1 and 2. Multiplying by a general polynomial series, admissible functions for the simply supported trapezoidal panel are obtained

$$w^1_{(x,y)} = F_{B(x,y)} \sum_{p=1}^{N_W} q_p x^{m^w_p} y^{n^w_p} \tag{17}$$

where the coefficients q_p are the generalized displacements. Substituting the expression for F_B, from Eq. (15), we can write

$$w^1_{(x,y)} = \sum_{p=1}^{N_W} q_p \cdot \sum_{i=1}^{3} \sum_{j=1}^{6} U_i V_j x^{(m^v_j + m^w_p)} y^{(n^u_i + n^v_j + n^w_p)} \tag{18}$$

The admissible functions are thus expressed in terms of simple polynomials, where the pth admissible function [Eq. (2)] is given by

$$f_{p(x,y)} = \sum_{i=1}^{3} \sum_{j=1}^{6} U_i V_j x^{(m^v_j + m^w_p)} y^{(n^u_i + n^v_j + n^w_p)} \tag{19}$$

Stiffness Matrix

Polynomial description of skin layer thicknesses in terms of the global x-y coordinates was given in Eqs. (10) and (11). This thickness distribution is for an entire wing box, or segments of the wing box. The panels analyzed for buckling are those trapezoidal skin segments defined by the supporting internal spar/rib array (Fig. 1). For each such panel containing N_L layers of fibers, the in-plane stiffness matrix $[A]$ can be expressed in terms of individual layer thicknesses and fiber orientation angles as

$$[A] = \sum_{i=1}^{N_L} \{[Q_0] + [Q_1]\cos 2\theta_i + [Q_2]\cos 4\theta_i + [Q_3]\sin 2\theta_i + [Q_4]\sin 4\theta_i\} \cdot t_{i(x,y)} \tag{20}$$

where the matrices $[Q_0]$ to $[Q_4]$ depend on material invariants U_{m1}, U_{m2}, U_{m3}, U_{m4}, U_{m5} and a general material matrix for a layer with fiber direction θ is

$$[Q] = \begin{bmatrix} U_{m1} & U_{m4} & 0 \\ U_{m4} & U_{m1} & 0 \\ 0 & 0 & U_{m5} \end{bmatrix} + U_{m2} \begin{bmatrix} 1 & 0 & 0 \\ 0 & -1 & 0 \\ 0 & 0 & 0 \end{bmatrix} \cos(2\theta) + U_{m3} \begin{bmatrix} 1 & -1 & 0 \\ -1 & 1 & 0 \\ 0 & 0 & -1 \end{bmatrix} \cos(4\theta) + \frac{U_{m2}}{2} \begin{bmatrix} 0 & 0 & 1 \\ 0 & 0 & 1 \\ 1 & 1 & 0 \end{bmatrix} \sin(2\theta) + U_{m3} \begin{bmatrix} 0 & 0 & 1 \\ 0 & 0 & -1 \\ 1 & -1 & 0 \end{bmatrix} \sin(4\theta) \tag{21}$$

Let a material and fiber orientation-dependent matrix $[\bar{\bar{Q}}(\theta_i)]$, a 3 × 3 matrix, be defined as

$$[\bar{\bar{Q}}(\theta_i)] = \{[Q_0] + [Q_1]\cos 2\theta_i + [Q_2]\cos 4\theta_i + [Q_3]\sin 2\theta_i + [Q_4]\sin 4\theta_i\} \tag{22}$$

The in-plane stiffness matrix $[A]$ can now be expressed in terms of the sizing design variables T^i_j and fiber directions, as a polynomial

$$[A] = \sum_{i=1}^{N_L} \sum_{k=1}^{N_i} [\bar{\bar{Q}}(\theta_i)] \cdot x^{(m^{ti}_k)} \cdot y^{(n^{ti}_k)} \cdot T^i_k \tag{23}$$

For unidirectional, orthotropic, or quasihomogeneous laminates[7,32,35] the in-plane and bending stiffness matrices are related through

$$[D] = [A](h^2/12) \tag{24}$$

Using Eq. (11) to express h^2 in terms of sizing-type design variables, double summation is needed. The indices $l1$ and $l2$ are used for summation of polynomial terms associated with each layer, as follows:

$$h_{(x,y)} = \sum_{i1=1}^{N_L} \sum_{l1=1}^{N_{i1}} T^{i1}_{l1} \cdot x^{(m^{ti1}_{l1})} \cdot y^{(n^{ti1}_{l1})} = \sum_{i2=1}^{N_L} \sum_{l2=1}^{N_{i2}} T^{i2}_{l2} \cdot x^{(m^{ti2}_{l2})} \cdot y^{(n^{ti2}_{l2})} \tag{25}$$

The bending stiffness matrix $[D]$ can now be written in polynomial form as

$$[D] = [A]\frac{h^2}{12} = \frac{1}{12} \sum_{i=1}^{N_L} [\bar{\bar{Q}}(\theta_i)] \sum_{i1=1}^{N_L} \sum_{i2=1}^{N_L} \sum_{k=1}^{N_i} \sum_{l1=1}^{N_{i1}} \sum_{l2=1}^{N_{i2}} \times \{T^i_k \cdot T^{i1}_{l1} \cdot T^{i2}_{l2} \cdot x^{(m^{ti}_k + m^{ti1}_{l1} + m^{ti2}_{l2})} y^{(n^{ti}_k + n^{ti1}_{l1} + n^{ti2}_{l2})}\} \tag{26}$$

The dependence of $[D]$ on the sizing design variables (thickness coefficients) and fiber angles is now expressed in explicit form. With the polynomial Ritz functions presented in Eqs. (2) and (19), and the stiffness matrix based Eq. (7), expressions for terms of the stiffness matrix in polynomial form can now be derived. Elements of the matrix $[F3]$ [Eq. (4)] in polynomial form are generated first, as follows: Second de-

Table 1 Constants U_i and V_j and their corresponding powers of x and y, associated with the admissible displacement series function F_B

j	V_j	m^v_j	n^v_j	i	U_i	n^u_i
1	V_1	0	0	1	U_1	0
2	V_2	1	0	2	U_3	1
3	V_3	0	1	3	U_3	2
4	V_4	2	0			
5	V_5	1	1			
6	V_6	0	2			

Table 2 Coefficients and powers of polynomial terms in the $[F_3]$ matrix

q, row of $[F_3]$ matrix	F^{qp}_{ij}, coefficient	mf^{qp}_{ij}, power of x	nf^{qp}_{ij}, power of y
1	$U_i V_j (m^v_j + m^w_p) \cdot (m^v_j + m^w_p - 1)$	$m^v_j + m^w_p - 2$	$n^u_i + n^v_j + n^w_p$
2	$U_i V_j (n^u_i + n^v_j + n^w_p) \cdot (n^u_i + n^v_j + n^w_p - 1)$	$m^v_j + m^w_p$	$n^u_i + n^v_j + n^w_p - 2$
3	$U_i V_j (m^v_j + m^w_p) \cdot (n^u_i + n^v_j + n^w_p)$	$m^v_j + m^w_p - 1$	$n^u_i + n^v_j + n^w_p - 1$

Note: If any of the power of x and y from columns three and four is less than zero, the corresponding F^{qp}_{ij} element is set to zero.

rivatives of the f_p [Eq. (19)] functions are expressed in polynomial form:

$$f_{p,xx} = \sum_{i=1}^{3} \sum_{j=1}^{6} U_i V_j (m_j^v + m_p^w)(m_j^v + m_p^w - 1) \times x^{(m_j^v + m_p^w - 2)} y^{(n_i^u + n_j^v + n_p^w)} \tag{27}$$

Note that $f_{p,xx} = 0$, if $m_j^v + m_p^w \leq 1$ (representing second derivatives of zero-order or first-order terms). Similarly,

$$f_{p,yy} = \sum_{i=1}^{3} \sum_{j=1}^{6} U_i V_j (n_i^u + n_j^v + n_p^w)(n_i^u + n_j^v + n_p^w - 1) \times x^{(m_j^v + m_p^w)} y^{(n_i^u + n_j^v + n_p^w - 2)} \tag{28}$$

where $f_{p,yy} = 0$, if $n_i^u + n_j^v + n_p^w \leq 1$. Finally,

$$2f_{p,xy} = 2 \sum_{i=1}^{3} \sum_{j=1}^{6} U_i V_j (m_j^v + m_p^w)(n_i^u + n_j^v + n_p^w) \times x^{(m_j^v + m_p^w - 1)} y^{(n_i^u + n_j^v + n_p^w - 1)} \tag{29}$$

In the last expression the term $f_{p,xy}$ is set to zero in two cases:

$$2f_{p,xy} = 0 \quad \text{if} \quad m_j^v + m_p^w = 0 \quad \text{or} \quad n_i^u + n_j^v + n_p^w = 0$$

The elements of the $[F3]$ matrix are, thus, all polynomials, and the q,p element of $[F_3]$ can be written as

$$F_{3q,p} = \sum_{i=1}^{3} \sum_{j=1}^{6} F_{ij}^{qp} x^{mf_{ij}^{qp}} y^{nf_{ij}^{qp}} \tag{30}$$

where the coefficients F_{ij}^{qp} and corresponding powers of x and y, mf_{ij}^{qp} and nf_{ij}^{qp}, respectively, are shown in the Table 2.

Equation (30) together with Eq. (26) are substituted into the equation for the stiffness matrix [Eq. (7)]. The r,sth term of the stiffness matrix is

$$K_{rs} = \sum_{a=1}^{3} \sum_{b=1}^{3} \iint (F_{3ar} D_{ab} F_{3bs})\, \mathrm{d}x\, \mathrm{d}y \tag{31}$$

and the final expression for the K_{rs} element in polynomial form is

$$K_{rs} = \sum_{a=1}^{3} \sum_{b=1}^{3} \sum_{\hat{i}=1}^{3} \sum_{\hat{j}=1}^{6} \sum_{\bar{i}=1}^{3} \sum_{\bar{j}=1}^{6} \sum_{i=1}^{N_L} \sum_{i1=1}^{N_L} \sum_{i2=1}^{N_L} \sum_{k=1}^{N_i} \sum_{l1=1}^{N_{i1}} \sum_{l2=1}^{N_{i2}} \frac{1}{12} \times F_{\hat{i},\hat{j}}^{a,r} F_{\bar{i},\bar{j}}^{b,s} \bar{\bar{Q}}_{a,b}(\theta_i) T_k^i T_{l1}^{i1} T_{l2}^{i2} \cdot \iint x^{(m_{rs})} y^{(n_{rs})}\, \mathrm{d}x\, \mathrm{d}y \tag{32}$$

where the powers of the x and y terms in the area integral are

$$m_{rs} = mf_{\hat{i},\hat{j}}^{a,r} + mf_{\bar{i},\bar{j}}^{b,s} + m_k^{i} + m_{l1}^{i1} + m_{l2}^{i2}$$

$$n_{rs} = nf_{\hat{i},\hat{j}}^{a,r} + nf_{\bar{i},\bar{j}}^{b,s} + n_k^{i} + n_{l1}^{i1} + n_{l2}^{i2}$$

All elements of the stiffness matrix are, thus, linear combinations of integrals over the panel's area of the form

$$I_{\mathrm{TR}(m,n)} = \iint_{\text{area}} x^m y^n\, \mathrm{d}x\, \mathrm{d}y \tag{33}$$

Note the explicit dependence on thickness coefficients and fiber directions. Dependence on panel shape is more complex. The coefficients U_i and V_j [Eqs. (16)] depend on the x, y positions of the vertices of the panel. These coefficients, in turn, determine the F coefficients in Table 2. In addition, the area integrals [Eq. (33)] depend on the shape of the panel, since the polynomial terms are defined in global (physical) coordinates, and the limits of integration change when the planform shape is changing. The integrations [Eq. (33)] can be carried out analytically, as shown in detail in Refs. 23, 25, and 27.

Geometric Stiffness Matrix

In-Plane Loads from Wing Box Stress Analysis

The geometric stiffness matrix in the Rayleigh–Ritz buckling analysis formulation for skin panels is given in Eq. (8), and it depends on the matrix $[F_2]$ [Eq. (3)], containing derivatives of the admissible functions, and the matrix $[N]$ containing the in-plane loads. In classical linear buckling analysis of the panel, these in-plane loads are assumed given, and they are determined by a separate stress analysis of the wing box, before the buckling analysis for the panel is carried out. In the case of wing structures, wing box stress analysis can be based on standard finite element techniques. In this case, in-plane forces along the sides of the panel are obtained by some functional approximation based on either nodal forces acting on nodes surrounding the panel, or in-plane stresses evaluated for the finite elements surrounding the panel. Alternatively, based on stress distribution in the panel, in-plane loads for buckling analysis can be evaluated throughout the panel, to be integrated over the area of the panel to obtain the matrix $[K_G]$ (Refs. 8–10, 12, 15–17, 33, and 34).

For preliminary design purposes, if the skin panels are small relative to the wing, buckling evaluation may be accurate enough if average N_x, N_y, and N_{xy} are used for the panel buckling analysis. These in-plane stresses are assumed constant throughout the panel in this case. This simplifies the integrations in Eq. (8), and makes it possible to use interaction formulas for fast approximate buckling analysis.[10,16,33]

When an equivalent plate modeling approach is used for the wing box analysis,[21–23] the in-plane skin stresses are obtained from the wing generalized displacements calculated in the wing box stress analysis stage. In the formulation used in Refs. 21–23 admissible Ritz functions for the wing box analysis are given as polynomials in x and y [the global coordinates used to define the planform of the wing and the shape of all panels (Fig. 1)]. In this case, the transverse displacement of the wing is

$$\bar{W}_{(x,y)} = \sum_{i=1}^{\bar{N}_w} x^{\bar{m}_i} y^{\bar{n}_i} \bar{q}_i \tag{34}$$

where a bar will associate variables with the wing box analysis. In Eq. (34), the powers $\bar{m}_i$, $\bar{n}_i$, and the number of terms $\bar{N}_w$ are known from the Ritz series used for the wing box displacement solution. The coefficients $\bar{q}_i$, are the generalized wing box displacements. Multiple load cases can be accounted for in the wing analysis, leading to different generalized displacement vectors $\{\bar{q}\}$.

In equivalent plate wing structural analysis based on classical plate theory,[21–23] the vertical displacement under loading is $\bar{W}_{(x,y)}$, and using Kirchoff's kinematics for a wing with a symmetric cross section, the engineering strains in the x and y directions are given by (Ref. 2, p. 19)

$$\begin{aligned} \overline{\varepsilon_x} &= \frac{\partial \bar{u}}{\partial x} = -z\bar{W}_{,xx} \\ \overline{\varepsilon_y} &= \frac{\partial \bar{v}}{\partial y} = -z\bar{W}_{,yy} \\ \overline{\gamma_{xy}} &= -2z\bar{W}_{,xy} \end{aligned} \tag{35}$$

Let the wing depth be given by $\bar{H}_{(x,y)}$. Then, when skins are thin compared to the depth, they can be assumed located at $z = \pm \bar{H}_{(x,y)}/2$. Focusing on the upper skin, in-plane strains are [Eqs. (35)]

$$\begin{Bmatrix} \bar{\varepsilon}_x \\ \bar{\varepsilon}_y \\ \bar{\gamma}_{xy} \end{Bmatrix} = -\frac{\bar{H}_{(x,y)}}{2} \begin{Bmatrix} \bar{W}_{,xx} \\ \bar{W}_{,yy} \\ 2\bar{W}_{,xy} \end{Bmatrix} \tag{36}$$

Now, in a polynomial-based formulation for the wing box, the depth of the wing is given in polynomial form

$$\bar{H}_{(x,y)} = \sum_{ih=1}^{Nh} \bar{H}_{ih} \cdot x^{(mh_{ih})} \cdot y^{(nh_{ih})} \tag{37}$$

Since the displacement $\bar{W}_{(x,y)}$ and the depth $\bar{H}_{(x,y)}$ are polynomial, it is evident [Eq. (36)], that skin strains due to wing deformation are polynomial too. There are a total of N_L layers, each with fiber direction θ_i, and thickness as described by a polynomial equation [Eq. (10)]. The in-plane skin stresses in each layer are obtained from the strains by [Eq. (22)]

$$\begin{Bmatrix} \bar{\sigma}_{xx} \\ \bar{\sigma}_{yy} \\ \bar{\sigma}_{xy} \end{Bmatrix}_i = [\bar{\bar{Q}}_{(\theta_i)}] \begin{Bmatrix} \bar{\varepsilon}_x \\ \bar{\varepsilon}_y \\ \bar{\gamma}_{xy} \end{Bmatrix} \tag{38}$$

The in-plane loads can now be found in terms of wing box displacements by integration through the thickness of the panel:

$$\begin{Bmatrix} N_x \\ N_y \\ N_{xy} \end{Bmatrix} = \int_z \begin{Bmatrix} \bar{\sigma}_{xx} \\ \bar{\sigma}_{yy} \\ \bar{\sigma}_{xy} \end{Bmatrix} \mathrm{d}z = \int_z [\bar{\bar{Q}}_{(\theta)}] \begin{Bmatrix} \bar{\varepsilon}_x \\ \bar{\varepsilon}_y \\ \bar{\gamma}_{xy} \end{Bmatrix} \mathrm{d}z$$

$$= -\frac{\bar{H}_{(x,y)}}{2} \cdot \int_z [\bar{\bar{Q}}_{(\theta)}]\, \mathrm{d}z \cdot \begin{Bmatrix} \bar{W}_{,xx} \\ \bar{W}_{,yy} \\ 2\bar{W}_{,xy} \end{Bmatrix} \tag{39}$$

leading to [Eqs. (20–23)]

$$\begin{Bmatrix} N_x \\ N_y \\ N_{xy} \end{Bmatrix} = -\frac{\bar{H}_{(x,y)}}{2} \cdot \sum_{i=1}^{NL} [\bar{\bar{Q}}_{(\theta_i)}] t_{i(x,y)} \cdot \begin{Bmatrix} \bar{W}_{,xx} \\ \bar{W}_{,yy} \\ 2\bar{W}_{,xy} \end{Bmatrix}$$

$$= -\frac{\bar{H}}{2} [A] \begin{Bmatrix} \bar{W}_{,xx} \\ \bar{W}_{,yy} \\ 2\bar{W}_{,xy} \end{Bmatrix} \tag{40}$$

We now turn to the derivatives of the wing displacement, in order to express Eq. (40) in terms of the generalized displacements $\{\bar{q}\}$ calculated for the wing box solution. We define a new vector $[\boldsymbol{\alpha}]$ of wing box curvatures as follows:

$$\{\boldsymbol{\alpha}\} = \begin{Bmatrix} \bar{W}_{,xx} \\ \bar{W}_{,yy} \\ 2\bar{W}_{,xy} \end{Bmatrix}$$

$$= \begin{bmatrix} \cdots & \bar{m}pw(\bar{m}pw - 1)x^{\bar{m}pw-2}y^{\bar{n}pw} & \cdots \\ \cdots & \bar{n}pw(\bar{n}pw - 1)x^{\bar{m}pw}y^{\bar{n}pw-2} & \cdots \\ \cdots & \bar{m}pw \cdot \bar{n}pw \cdot x^{\bar{m}pw-1}y^{\bar{n}pw-1} & \cdots \end{bmatrix} \begin{Bmatrix} \cdot \\ \cdot \\ \bar{q}_{pw} \\ \cdot \end{Bmatrix} \tag{41}$$

where pw is an index for the pth element in the wing Ritz series. There are $\bar{N}_w$ terms in the Ritz series for wing displacement [Eq. (34)]. The matrix associated with $\{\boldsymbol{\alpha}\}$ in Eq. (41) is, thus, 3 by $\bar{N}_w$. Each element of this matrix is of the form $W_{qw,pw} \cdot x^{(\bar{m}_{qw,pw})} \cdot y^{(\bar{n}_{qw,pw})}$, where the coefficient $W_{qw,pw}$, and powers of x and y, $\bar{m}_{qw,pw}$ and $\bar{n}_{qw,pw}$, respectively, are described in Table 3. When the index qw denotes the row of the matrix (its values varying from 1 to 3) and the index pw specifies terms of the polynomial displacement series for the wing box (varying from 1 to $\bar{N}_w$), then [Eqs. (40)], the in-plane load N_x for the panel can be expressed in polynomial form as

$$N_x = -\frac{\bar{H}}{2} \sum_{qw=1}^{3} A_{1,qw} \cdot \alpha_{qw} = -\frac{\bar{H}}{2} \sum_{qw=1}^{3} A_{1,qw}$$

$$\times \sum_{pw=1}^{\bar{N}_w} W_{qw,pw} x^{\bar{m}_{qw,pw}} y^{\bar{n}_{qw,pw}} \bar{q}_{pw}$$

leading to

$$N_x = -\frac{\bar{H}}{2} \sum_{qw=1}^{3} \sum_{pw=1}^{\bar{N}_w} A_{1,qw} \cdot W_{qw,pw} x^{\bar{m}_{qw,pw}} y^{\bar{n}_{qw,pw}} \bar{q}_{pw} \tag{42}$$

Similarly, the expressions for N_y and N_{xy} can be derived:

$$N_y = -\frac{\bar{H}}{2} \sum_{qw=1}^{3} \sum_{pw=1}^{\bar{N}_w} A_{2,qw} \cdot W_{qw,pw} x^{\bar{m}_{qw,pw}} y^{\bar{n}_{qw,pw}} \bar{q}_{pw} \tag{43}$$

$$N_{xy} = -\frac{\bar{H}}{2} \cdot 2 \sum_{qw=1}^{3} \sum_{pw=1}^{\bar{N}_w} A_{3,qw} W_{qw,pw} x^{\bar{m}_{qw,pw}} y^{\bar{n}_{qw,pw}} \bar{q}_{pw}$$

$$= -\bar{H} \sum_{qw=1}^{3} \sum_{pw=1}^{\bar{N}_w} A_{3,qw} W_{qw,pw} x^{\bar{m}_{qw,pw}} y^{\bar{n}_{qw,pw}} \bar{q}_{pw} \tag{44}$$

Now the polynomial expression for wing depth [Eq. (37)] can be substituted into Eqs. (42–44). The general expression for terms of the $[N]$ matrix

$$[N] = \begin{bmatrix} N_x & N_{xy} \\ N_{xy} & N_y \end{bmatrix}$$

is

$$N_{pp,qq} = -\frac{1}{2} \sum_{ih=1}^{Nh} \sum_{qw=1}^{3} \sum_{pw=1}^{\bar{N}_w} A_{ppp,qw} \cdot W_{qw,pw} \cdot H_{ih} \cdot x^{(mih + \bar{m}_{qw,pw})}$$

$$\times y^{(n_{ih} + \bar{n}_{qw,pw})} \cdot \bar{q}_{pw} \tag{45}$$

The indices pp and qq can be either 1 or 2. Note

$$\begin{gathered} \text{If } pp = 1 \text{ and } qq = 1, \text{ then } A_{ppp,qw} = A_{1,qw} \\ \text{If } pp = 2 \text{ and } qq = 2, \text{ then } A_{ppp,qw} = A_{2,qw} \\ \text{When } pp \neq qq,\ A_{ppp,qw} = 2A_{3,qw} \end{gathered} \tag{46}$$

The polynomial expression for the $[A]$ matrix [Eq. (23)] is now used:

$$N_{pp,qq} = -\frac{1}{2} \sum_{ih=1}^{Nh} \sum_{qw=1}^{3} \sum_{pw=1}^{\bar{N}_w} \sum_{i=1}^{NL} \sum_{k=1}^{N_i} \{\bar{\bar{Q}}_{ppp,qw}(\theta_i) \cdot W_{qw,pw}$$

$$\times H_{ih} \cdot T_k^i \cdot \bar{q}_{pw} x^{(m_{ih} + mt_k^i + \bar{m}_{qw,pw})} \cdot y^{(n_{ih} + nt_k^i + \bar{n}_{qw,pw})}\} \tag{47}$$

Table 3 Elements of the matrix $\{\alpha\}$; coefficients and powers of x and y

	$W_{qw,pw}$	$\bar{m}_{qw,pw}$	$\bar{n}_{qw,pw}$
$qw = 1$, row 1 of the matrix	$\bar{m}_{pw}(\bar{m}_{pw} - 1)$	$\bar{m}_{pw} - 2$	$\bar{n}_{pw}$
$qw = 2$, row 2 of the matrix	$\bar{n}_{pw}(\bar{n}_{pw} - 1)$	$\bar{m}_{pw}$	$\bar{n}_{pw} - 2$
$qw = 3$, row 3 of the matrix	$\bar{m}_{pw}\bar{n}_{pw}$	$\bar{m}_{pw} - 1$	$\bar{n}_{pw} - 1$

where the index ppp means the following:

$$
\begin{aligned}
&\text{If } pp = 1 \text{ and } qq = 1, \text{ then } \bar{\bar{Q}}_{ppp,qw} = \bar{\bar{Q}}_{1,qw} \\
&\text{If } pp = 2 \text{ and } qq = 2, \text{ then } \bar{\bar{Q}}_{ppp,qw} = \bar{\bar{Q}}_{2,qw} \\
&\quad \text{When } pp \neq qq, \ \bar{\bar{Q}}_{ppp,qw} = 2\bar{\bar{Q}}_{3,qw}
\end{aligned}
\tag{48}
$$

The matrix $[N]$ can then be expressed as a polynomial in x and y according to Eq. (48). This equation shows how $[N]$ depends on the wing box solution, the depth of the wing, the thickness coefficients for layers in the panel, material properties, and fiber directions. Of course, the wing solution $\{\bar{q}\}$, also depends on depth, thickness of layers, fiber directions, and material properties. These affect the stiffness matrix of the wing as described in Refs. 21–23 and 25–27. It should be emphasized again, that polynomial in-plane loads for the buckling analysis, can be obtained in a similar manner from wing box analysis based on first-order shear deformation plate theory[27] or from finite element results, when skin stresses are approximated by polynomials using least-square fitting.[35]

Geometric Stiffness Matrix

Based on the Ritz polynomial functions [Eq. (19)], the matrix $[F2]$, needed for evaluation of the geometric stiffness matrix [Eq. (8)], can be written in polynomial form as follows:

Derivatives with respect to x and y of the Ritz functions are

$$
f_{p,x} = \sum_{i=1}^{3}\sum_{j=1}^{6} U_i V_j (m_p^w + m_j^v) \cdot x^{(m_p^w + m_j^v - 1)} \cdot y^{(n_p^w + n_i^u + n_j^v)} \tag{49}
$$

$$
f_{p,y} = \sum_{i=1}^{3}\sum_{j=1}^{6} U_i V_j (n_p^w + n_i^u + n_j^v) \cdot x^{(m_p^w + m_j^v)} \cdot y^{(n_p^w + n_i^u + n_j^v - 1)} \tag{50}
$$

Thus, the element q, p of the matrix $[F_2]$ is of the form

$$
F_{2(q,p)} = \sum_{i=1}^{3}\sum_{j=1}^{6} \bar{F}_{2i,j}^{q,p} \cdot x^{(mf2_{i,j}^{q,p})} \cdot y^{(nf2_{i,j}^{q,p})} \tag{51}
$$

The coefficients $\bar{F}_{2i,j}^{q,p}$ and powers of x and y, $mf2_{i,j}^{q,p}$ and $nf2_{i,j}^{q,p}$, defining the elements of the $[F_2]$ matrix, are described in Table 4. Elements of the matrix $[K_G]$ can now be expressed in polynomial form as follows:

$$
K_{Gr,s} = \iint \sum_{a=1}^{2}\sum_{b=1}^{2} F_{2a,r} N_{a,b} F_{2b,s} \, dx \, dy \tag{52}
$$

The indices r and s identify terms in the panel Ritz displacement series for the panel. Using polynomial expressions for $[F_2]$ and $[N]$, the r, s element of $[K_G]$ is written as

$$
\begin{aligned}
K_{Gr,s} = &-\frac{1}{2} \sum_{a=1}^{2}\sum_{b=1}^{2}\sum_{i=1}^{3}\sum_{j=1}^{6}\sum_{\bar{i}=1}^{3}\sum_{\bar{j}=1}^{6}\sum_{ih=1}^{Nh}\sum_{qw=1}^{3}\sum_{pw=1}^{\bar{N}_w} \\
&\times \sum_{it=1}^{NL}\sum_{k=1}^{Nt} \bar{F}_{2i,j}^{a,r} \cdot \bar{F}_{2\bar{i},\bar{j}}^{b,s} \cdot \bar{\bar{Q}}_{ppp,qw}(\theta_{it}) \cdot W_{qw,pw} \cdot H_{ih} \cdot T_k^{it} \\
&\times \bar{q}_{pw} \cdot \iint x^{(mG_{r,s})} y^{(nG_{r,s})} \, dx \, dy
\end{aligned}
\tag{53}
$$

where

$$
\begin{aligned}
mG_{r,s} &= mf2_{i,j}^{a,r} + mf2_{\bar{i},\bar{j}}^{b,s} + m_{ih} + mt_k^{it} + \bar{m}_{qw,pw} \\
nG_{r,s} &= nf2_{i,j}^{a,r} + nf2_{\bar{i},\bar{j}}^{b,s} + n_{ih} + nt_k^{it} + \bar{n}_{qw,pw}
\end{aligned}
\tag{54}
$$

The index ppp used in $\bar{\bar{Q}}_{ppp,qw}(\theta_{it})$ is defined in Eq. 48. As in the case of the stiffness matrix $[K]$, the geometric stiffness matrix is represented as summation of surface integrals of polynomial terms calculated over the area of the panel. Integrals of the same family $I_{TR}(m, n)$ are used [Eq. (33)], where the powers of x and y are determined from Eq. (54). Evaluation of these integrals is discussed in detail in Refs. 23, 25, and 27, and for trapezoidal panels it can be done analytically using the same subroutines used in the wing analysis and panel stiffness analysis.

Further Discussion of Integration with Wing Structural Analysis

Recall that the results of the wing analysis affect buckling analysis of the panel through the in-plane matrix $[N]$. This matrix is obtained by integrating skin stresses (due to wing deformation) through the thickness of the skin, and the resulting N_x, N_y, and N_{xy} are functions of x and y as evident in Eqs. (45–48). Now, while equivalent plate wing structural analysis leads to good skin stress predictions in stiff, low AR wings,[21–23] still equilibrium is not guaranteed for isolated skin panels. Thus, the in-plane loads [as given by Eq. (47)] are generally not in equilibrium. [This problem is not encountered when wing analysis is based on the finite element method (FEM), when in-plane loading on the circumference of an isolated panel is determined from nodal forces on that circumference.]

One way to avoid this difficulty and simplify buckling analysis of panels is to use an average in-plane loading to be assumed constant over the panel.[33] If point (x_0, y_0) inside the panel is used to evaluate these average in-plane loads, then the elements of $[N]$ become [Eq. (47)]

$$
\begin{aligned}
N_{pp,qq} = &-\frac{1}{2} \sum_{ih=1}^{Nh}\sum_{qw=1}^{3}\sum_{pw=1}^{\bar{N}_w} A_{ppp,qw} \cdot W_{qw,pw} \\
&\times H_{ih} \cdot x_0^{(m_{ih} + \bar{m}_{qw,pw})} \cdot y_0^{(n_{ih} + \bar{n}_{qw,pw})} \cdot \bar{q}_{pw}
\end{aligned}
\tag{55}
$$

The expression for elements of the geometric stiffness matrix [Eq. (53)] has to be modified, since terms including x_0 and y_0 become constant for the area integration, and can be taken out of the integral:

$$
\begin{aligned}
K_{Gr,s} = &-\frac{1}{2} \sum_{a=1}^{2}\sum_{b=1}^{2}\sum_{i=1}^{3}\sum_{j=1}^{6}\sum_{\bar{i}=1}^{3}\sum_{\bar{j}=1}^{6}\sum_{ih=1}^{Nh}\sum_{qw=1}^{3}\sum_{pw=1}^{\bar{N}_w} \\
&\times \sum_{it=1}^{NL}\sum_{k=1}^{Nt} \bar{F}_{2i,j}^{a,r} \cdot \bar{F}_{2\bar{i},\bar{j}}^{b,s} \cdot \bar{\bar{Q}}_{ppp,qw}(\theta_{it}) \cdot W_{qw,pw} \\
&\times H_{ih} \cdot T_k^{it} \cdot \bar{q}_{pw} \cdot x_0^{(m_{ih} + \bar{m}_{qw,pw})} \cdot y_0^{(n_{ih} + \bar{n}_{qw,pw})} \\
&\times \iint \{ x^{(mf2_{i,j}^{a,r} + mf2_{\bar{i},\bar{j}}^{b,s} + mt_k^{it})} \cdot y^{(nf2_{i,j}^{a,r} + nf2_{\bar{i},\bar{j}}^{b,s} + nt_k^{it})} \, dx \, dy \}
\end{aligned}
\tag{56}
$$

Analytic Sensitivities

Stiffness Matrix Sensitivities

With the explicit expression of stiffness matrix elements (in terms of thickness, fiber directions and shape of the panel)

Table 4 Coefficients and powers of terms of the $[F_2]$ matrix

	$\bar{F}_{2i,j}^{q,p}$	$mf2_{i,j}^{q,p}$	$nf2_{i,j}^{q,p}$
$q = 1$, row 1 of $[F_2]$ matrix	$U_i V_j (m_p^w + m_j^v)$	$m_p^w + m_j^v - 1$	$n_p^w + n_i^u + n_j^v$
$q = 2$, row 2 of $[F_2]$ matrix	$U_i V_j (n_p^w + n_i^u + n_j^v)$	$m_p^w + m_j^v$	$n_p^w + n_i^u + n_j^v - 1$

available in the form of Eq. (32), it is straightforward to obtain sensitivities analytically. Three types of sensitivities can be evaluated: 1) sensitivities with respect to thickness design variables, T_k^i; 2) sensitivities with respect to layer orientation angle, θ_i; and 3) sensitivities with respect to planform shape variables.

Stiffness Sensitivities with Respect to Thickness Design Variables T_k^i

Planform shape variables and orientation angles are fixed in this case. The thickness coefficients T_k^i appear in the expression for the stiffness matrix [Eq. (32)] explicitly in a triple summation over the indices k, 11, and 12. Sensitivity is then obtained by direct differentiation, noting that if the design variable involved is T_r^q, then $\partial T_k^i/\partial T_r^q = 1$ only when $i = q$ and $k = r$; otherwise, the derivative is zero.

Sensitivities with Respect to Fiber Direction θ_i

Now the planform is fixed and thickness is fixed. The angle θ_i represents the direction of fibers in the ith layer, and the stiffness matrix K_{rs} depends on θ_i through elements of the matrix $[\bar{\bar{Q}}(\theta_i)]$ [Eq. (22)]. The derivative of each term in the stiffness matrix will be calculated in the following manner. In the summation [Eq. (32)] over $i = 1$ to N_L, all matrices $[\bar{\bar{Q}}(\theta_i)]$ are set to zero, except the matrix $[\bar{\bar{Q}}(\theta_i)]$ corresponding to the θ_i variable considered. This particular $[\bar{\bar{Q}}(\theta_i)]$ is replaced [in Eq. (32)] by the following expression [Eq. (22)]:

$$\frac{\partial \bar{\bar{Q}}_{(\theta i)}}{\partial \theta_i} = -2[Q_1]\sin 2\theta_i - 4[Q_2]\sin 4\theta_i + 2[Q_3]\cos 2\theta_i + 4[Q_4]\cos 4\theta_i \tag{57}$$

Equation (32) is, thus, used for the sensitivity of the stiffness term, with the derivative Eq. (57) replacing $[\bar{\bar{Q}}(\theta_i)]$.

Stiffness Sensitivities with Respect to Panel Planform Variables y_L, y_R, x_{FL}, x_{FR}, x_{AL}, and x_{AR} (Fig. 1)

Thickness coefficients and orientation angles are held fixed. The terms K_{rs} of the stiffness matrix depend on the planform through matrix $[F_3]$ [Eq. (30) and Table 2] and the integrals $I_{\mathrm{TR}(m,n)}$ [Eq. (33)]. Coefficients U_i and V_j are defined through expressions (16) and (18). If x is any planform design variable, then

$$\frac{\partial F_{ij}^{qp}}{\partial x} = \left(\frac{\partial U_i}{\partial x} V_j + U_i \frac{\partial V_j}{\partial x}\right) \cdot (\text{integers in Table 2}) \tag{58}$$

Through Eqs. (16), the terms U_i and V_j are given explicitly in terms of the panel shape design variables. Analytic sensitivities of U_i and V_j are obtained by direct differentiation.[36] For example, derivatives with respect to x_{FR} are calculated as follows:

$$\frac{\partial U_1}{\partial x_{FR}} = \frac{\partial U_2}{\partial x_{FR}} = \frac{\partial U_3}{\partial x_{FR}} = \frac{\partial V_4}{\partial x_{FR}} = 0$$

$$\frac{\partial V_1}{\partial x_{FR}} = \frac{-y_L}{y_R - y_L} R_A$$

$$\frac{\partial V_2}{\partial x_{FR}} = \frac{-y_L}{y_R - y_L}$$

$$\frac{\partial V_3}{\partial x_{FR}} = \frac{-y_L}{y_R - y_L} \cdot S_A + R_A \cdot \frac{1}{y_R - y_L}$$

$$\frac{\partial V_5}{\partial x_{FR}} = \frac{1}{y_R - y_L}$$

$$\frac{\partial V_6}{\partial x_{FR}} = \frac{1}{y_R - y_L} \cdot S_A$$

The derivatives of the terms F_{ij}^{qp} can now be prepared [Eq. (30), Table 2]. The tables for the derivatives $\partial I_{\mathrm{TR}}/\partial x$ are prepared using Refs. 23 and 25. It should be noted that in evaluating the shape derivatives of these integrals there is no need for more integrations over the panel's area. The shape sensitivities of the area integrals are linear combinations of other members of the same table of integrals, a table already available from the analysis step.

After collecting all the information necessary, one can calculate the derivative of the term K_{rs} as follows:

$$\frac{\partial K_{rs}}{\partial x} = \sum_{a=1}^{3} \sum_{b=1}^{3} \sum_{i=I}^{3} \sum_{j=1}^{6} \sum_{i=1}^{3} \sum_{j=1}^{6} \sum_{i=1}^{N_L} \sum_{i1=1}^{N_L} \sum_{i2=1}^{N_L} \sum_{k=1}^{N_i} \sum_{l1=1}^{N_{i1}} \sum_{l2=1}^{N_{i2}} \frac{1}{12} \times \left\{ \left[\frac{\partial F_{i,j}^{a,r}}{\partial x} F_{i,j}^{b,s} + F_{i,j}^{a,r} \frac{\partial F_{i,j}^{b,s}}{\partial x} \right] \cdot \bar{\bar{Q}}_{a,b}(\theta_i) T_k^i \cdot T_{l1}^{i1} \cdot T_{l2}^{i2} \cdot I_{\mathrm{TR}(m,n)} + F_{i,j}^{a,r} \cdot F_{i,j}^{b,s}\, \bar{\bar{Q}}_{a,b}(\theta_i) T_k^i T_{l1}^{i1} T_{l2}^{i2} \cdot \frac{\partial I_{\mathrm{TR}(m,n)}}{\partial x} \right\} \tag{59}$$

Geometric Stiffness Matrix Sensitivities

Geometric Stiffness Sensitivities with Respect to Thickness Design Variables T_k^{it}

The design variable in this case is the kth coefficient in the polynomial thickness series for the ith layer. Examination of Eqs. (53) and (54) reveals that the geometric stiffness matrix is explicitly linear in the thickness coefficients T_k^{it}. It is, of course, also dependent on those coefficients via the wing box solution $\{\bar{q}\}$, unless it is assumed that in-plane loads $[N]$ do not change. Differentiation of Eq. (53), using Eq. (33) leads to

$$\frac{\partial K_{Gr,s}}{\partial T_k^{it}} = -\frac{1}{2} \sum_{a=1}^{2} \sum_{b=1}^{2} \sum_{i=1}^{3} \sum_{j=1}^{6} \sum_{i=1}^{3} \sum_{j=1}^{6} \sum_{ih=1}^{N_h} \sum_{qw=1}^{3} \sum_{pw=1}^{\bar{N}_w} \sum_{R=1}^{N_L} \sum_{S=1}^{N_{ti}} \times \bar{F}_{2i,j}^{a,r} \cdot \bar{F}_{2i,j}^{b,s} \cdot \bar{\bar{Q}}_{ppp,qw(\theta_{it})} \cdot W_{qw,pw} \times H_{ih} \left[\Gamma_{k,S}^{it,R} \cdot \bar{q}_{pw} + T_S^R \cdot \frac{\partial \bar{q}_{pw}}{\partial T_k^{it}} \right] \cdot I_{\mathrm{TR}}(mG_{r,s}, nG_{r,s}) \tag{60}$$

where $\Gamma_{k,S}^{it,R}$ is equal to 1 only when $it = R$ and $k = S$. Otherwise, it is zero.

Geometric Stiffness Sensitivities with Respect to Fiber Direction θ_{it}

Layer orientations affect the geometric stiffness matrix through the material matrices $\bar{\bar{Q}}_{ppp,qw}(\theta_{it})$ and the wing box generalized displacements $\{\bar{q}\}$. The analytic sensitivity with respect to fiber direction in a given layer is

$$\frac{\partial K_{Gr,s}}{\partial \theta_{it}} = -\frac{1}{2} \sum_{a=1}^{2} \sum_{b=1}^{2} \sum_{i=1}^{3} \sum_{j=1}^{6} \sum_{i=1}^{3} \sum_{j=1}^{6} \sum_{ih=1}^{N_h} \sum_{qw=1}^{3} \sum_{pw=1}^{\bar{N}_w} \sum_{itt=1}^{N_L} \sum_{k=1}^{N_{ti}} \times \bar{F}_{2i,j}^{a,r} \cdot \bar{F}_{2i,j}^{b,s} \cdot \left[\frac{\partial \bar{\bar{Q}}_{ppp,qw}(\theta_{itt})}{\partial \theta_{it}} \cdot \bar{q}_{pw} + \bar{\bar{Q}}_{ppp,qw}(\theta_{itt}) \cdot \frac{\partial \bar{q}_{pw}}{\partial \theta_{it}} \right] \times W_{qw,pw} H_{ih} \cdot T_k^{it} \cdot I_{\mathrm{TR}}(mG_{r,s}, nG_{r,s}) \tag{61}$$

Geometric Stiffness Sensitivities with Respect to Planform Variables y_L, y_R, x_{FL}, x_{FR}, x_{AL}, and x_{AR}

Thickness coefficients and orientation angles are held fixed. The geometric stiffness matrix K_G depends on the planform variables through U_i and V_j terms [Eqs. (15) and (16)] in $\bar{F}_{2i,j}^{a,r}$ and $\bar{F}_{2ii,jj}^{b,s}$ [Table 4 and Eq. (51)]. There is also a dependence on the area integrals I_{TR} [Eq. (33)], since those are evaluated over the planform shape of the panel. Thus,

$$\frac{\partial K_{Gr,s}}{\partial x} = -\frac{1}{2}\sum_{a=1}^{2}\sum_{b=1}^{2}\sum_{i=1}^{3}\sum_{j=1}^{6}\sum_{i=1}^{3}\sum_{j=1}^{6}\sum_{ih=1}^{N_h}\sum_{qw=1}^{3}\sum_{pw=1}^{\bar{N}_w}\sum_{it=1}^{N_L}\sum_{k=1}^{N_{ti}} \times (\bar{Q}_{ppp.qw(\theta_{it})}\cdot W_{qw,pw}\cdot H_{ih}\cdot T_k^{it}) \times\left\{\left[\frac{\partial \bar{F}_{2i,j}^{a,r}}{\partial x}\bar{F}_{2i,j}^{b,s} + \bar{F}_{2i,j}^{a,r}\frac{\partial \bar{F}_{2i,j}^{b,s}}{\partial x}\right]\cdot \bar{q}_{pw} I_{\mathrm{TR}(m,n)} + \bar{F}_{2i,j}^{a,r}\bar{F}_{2i,j}^{b,s}\cdot\left[\bar{q}_{pw}\frac{\partial I_{\mathrm{TR}(m,n)}}{\partial x} + \frac{\partial \bar{q}_{pw}}{\partial x} I_{\mathrm{TR}(m,n)}\right]\right\} \tag{62}$$

where x represents any of the planform variables, and the powers of integrands in $I_{\mathrm{TR}(m,n)}$ are $m = mG_{r,s}$ and $n = nG_{r,s}$ [Eqs. (54)]. In Eq. (62) it is assumed that overall wing planform is fixed, and panels are changing shape and location due to moving of control surfaces, ribs, and spars. If overall planform shape of the wing is changing, then derivatives of the wing depth coefficients with respect to the shape design variables, $\partial H_{ih}/\partial x$, must be added, since the wing depth is defined in global x, y coordinates [Eq. (37)].

It is clear, examining the analytic sensitivities of stiffness and geometric stiffness derived in the previous sections, that all involve area integrals of polynomial terms over the panel's area. Since members of the family of integrals $I_{\mathrm{TR}(m,n)}$ are generated for the analysis stage, there is no need to generate them again for the sensitivity calculation stage. No numerical integration is needed, therefore, for either analysis or sensitivity calculations. This is similar to the process by which analytic sensitivities are obtained for the wing box analysis.[25] A table of area integrals over the wing surface has to be generated once (using the same analytic formulas used here for the panel). The integrals are subsequently used for wing box analysis and sensitivities.

Of course, when the wing changes shape, panels change shape too. There is linking, therefore, between overall wing planform design variables and panel vertex locations. This linking has to be accounted for in the sensitivity computations when overall wing/panel shapes are changing.

When constant in-plane load matrix $[N]$ is assumed for the panel buckling analysis, and when it is based on evaluation of in-plane loads at a point (x_0, y_0) on the panel [Eqs. (55) and (56)], then when shape sensitivities are required, the motion of point (x_0, y_0) when the panel changes shape has to be taken into account.

Eigenvalue Sensitivities

Now that the sensitivities of the $[K]$ and $[K_G]$ matrices ($\partial K_{Gr,s}/\partial x$ and $\partial K_{r,s}/\partial x$) are available analytically, the sensitivity of buckling eigenvalues, and, hence, the sensitivity of buckling constraints is given by

$$\frac{\partial g}{\partial x} = -\frac{\partial \lambda}{\partial x} = \frac{\{\phi\}^T\left(\dfrac{\partial[K]}{\partial x} + \lambda\dfrac{\partial[K_G]}{\partial x}\right)\{\phi\}}{\{\phi\}^T[K_G]\{\phi\}} \tag{63}$$

This analytic sensitivity can be used to construct direct, reciprocal, or hybrid approximations of the constraint.[37] Alternatively, the sensitivities of $[K]$ and $[K_G]$ can be used in a Rayleigh quotient approximation,[38,39] where, based on direct or reciprocal approximations, approximate stiffness $[K^{\mathrm{aprx}}]$ and geometric stiffness $[K_G^{\mathrm{aprx}}]$ matrices are constructed. In this case

$$g \approx 1 - \lambda^{\mathrm{aprx}} \approx 1 + \{\phi\}^T[K^{\mathrm{aprx}}]\{\phi\}/\{\phi\}^T[K_G^{\mathrm{aprx}}]\{\phi\} \tag{64}$$

Test Cases and Results

To assess the new capability, test cases were chosen to address the following issues: 1) convergence rate with increased polynomial order (fast convergence using low-order polynomial Ritz functions is important not only to avoid ill conditioning, but also to reduce computational resources needed for design optimization); 2) accuracy of analysis results for isotropic and anisotropic panels of general shape (rectangular, skewed, and triangular shapes were studied); 3) reliability of analytic sensitivities and accuracy of finite difference derivatives; 4) quality of conventional approximation techniques based on first-order sensitivity analysis in the presence of shape variations; and 5) integration of wing box structural analysis with panel buckling analysis for fast structural analysis of airplane wings.

Analysis results from Ref. 3 are used to test accuracy and convergence rate of the present technique in the case of rectangular anisotropic panels. Simply supported, angle ply laminates made of 20 plies of DLP material[3] with $a = 5$ in., $b = 10$ in., and combined in-plane loading consisting of $N_x = 1$, $N_y = 1$, and $N_{xy} = 1$, are considered. Figure 2 shows convergence of the buckling load (the critical eigenvalue) as a function of the order of polynomial Ritz series N_w [Eq. (17)]. Figure 3 shows critical buckling eigenvalues, calculated with $N_w = 4$ (15-term complete polynomial), for cases in which the fiber orientation angle varies. Good accuracy and fast convergence are demonstrated. With only 6 terms (order 2) the present results are only within 3% error of Ref. 3 results. For automated synthesis, where the need to have very fast analysis and sensitivity results is critical, this fast convergence makes it possible to use low-order models without sacrificing accuracy too much.

Skewed geometries with isotropic simply supported panels are examined next, and results are compared to those of Ref. 20. Figure 4 shows critical buckling eigenvalues for isotropic plates with various skew angles. The a/b ratio for the plates is 1, and the thickness over b ratio is 0.001. All aluminum

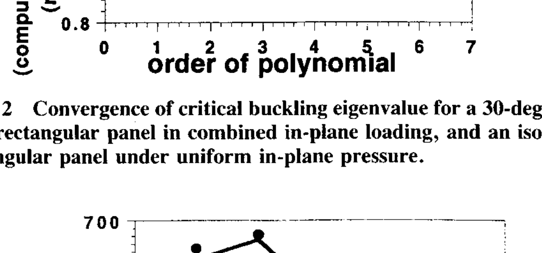

Fig. 2 Convergence of critical buckling eigenvalue for a 30-deg angle ply rectangular panel in combined in-plane loading, and an isotropic triangular panel under uniform in-plane pressure.

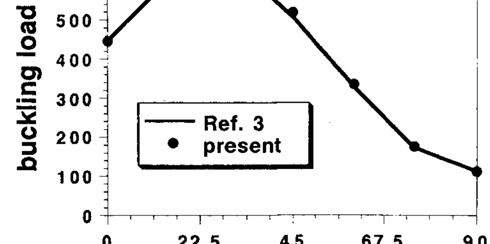

Fig. 3 Critical buckling eigenvalues for rectangular angle-ply panels.[3]

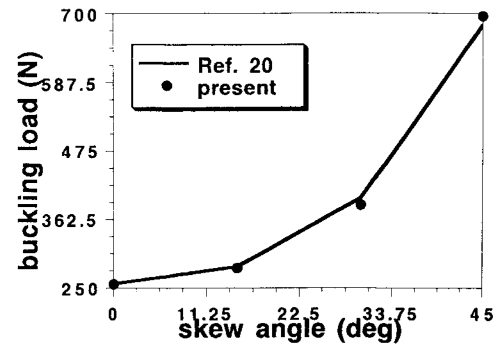

Fig. 4 Critical buckling loads for isotropic skewed panels.

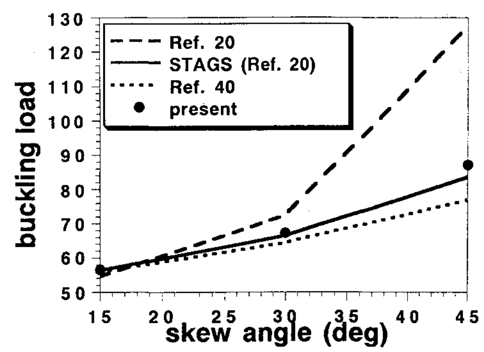

Fig. 5 Critical buckling loads for anisotropic skewed panels.

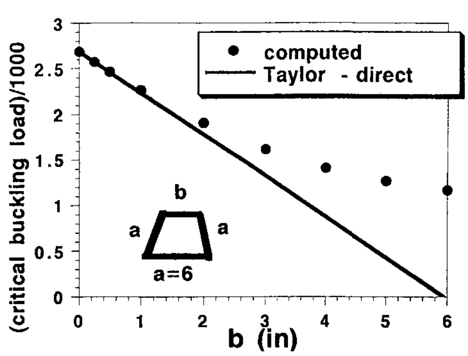

Fig. 6 Critical buckling load for trapezoidal isotropic panels of varying shape.

plates are analyzed with $a = b = 1$ m. Uniaxial compression of $N_x = 1$ is applied.

In Fig. 5, the combined effects of skew angle and anisotropy are examined, and the present results are compared to Ritz and finite element results from Ref. 20, and to results from Ref. 40. Orthotropic panels with $a = b = 1$ m, thickness of 0.001 m, a ratio of $D11/D22 = 5$ and $D66/D22 = 0.5$, are examined. Using the lay-up, thickness, and material distributions allowed in the present analysis, equivalent panels are created to match those in Refs. 20 and 40. Compressive in-plane loads of $N_x = N_y = 1$ and a shear load of $N_{xy} = 0.5$ were applied. Accuracy of the present results, obtained with a 15-term Ritz polynomial [Eq. (17)], is good, and the effects of anisotropy and skew angle present no difficulty.

Buckling results for a simply supported aluminum symmetric trapezoidal panel, in which one of the sides shrinks in size, are shown in Fig. 6. Uniform in-plane compression ($N_x = N_y = 1$) is applied. Starting with a rectangular geometry, the figure shows how the critical buckling eigenvalue varies until the trapezoid becomes a triangle. With analytic shape sensitivity with respect to the trapezoid's upper side (obtained as described in this article), direct Taylor series approximations are constructed[37] and shown in the figure. The reference design used is the triangular design (upper $b = 0$). The present capability is fast [10 Ritz terms are used in Eq. (17)] and reliable in both analysis and sensitivity computations.

Accuracy, behavior sensitivity, and Taylor-series approximations for triangular panels of variable shape are shown in Figs. 2 and 7. Simply supported equilateral aluminum panels are analyzed for buckling, and the effect of varying ratio of altitude to base (a/b) is examined.[33] A typical convergence study for the case of an equilateral panel is shown in Fig. 2. Fast convergence is achieved to the result of Ref. 41, allowing the use of low-order models in subsequent studies. In Fig. 7, the variation of critical buckling eigenvalue with changes in a/b is shown. "Exact" results (obtained with 10 Ritz terms) are shown, as well as direct and reciprocal Taylor series approximations based on analysis and analytical sensitivity at the reference design ($a/b = 1$). Rayleigh quotient approximations (RQA) are also shown. They perform quite well for values of a/b greater than the reference value. However, when a/b is smaller than the reference value, both RQA approximations fail beyond a 10% move limit. This approximation failure is similar to the problems encountered when aeroservoelastic poles are approximated in wing planform shape synthesis based on the equivalent plate approach.[42] Resolution of this problem and improved approximations for the case of planform shape variations, is beyond the scope of the present article, and will be reported separately.

Figure 8 shows comparisons of first-order finite difference sensitivities to analytic sensitivities obtained with the present formulation. The rectangular panel used for the convergence studies of Fig. 2 is used here. Design variables are thickness, fiber angle, and two shape variables, *YR* and *XFR* (see Fig. 1). Results were obtained with 10 Ritz terms. As can be seen, reliable finite difference sensitivities can be obtained with step sizes between 0.001–0.1%. It should be recognized that when simple polynomials are used for Ritz wing box analysis,[25] ill conditioning can lead to situations in which no reliable first-

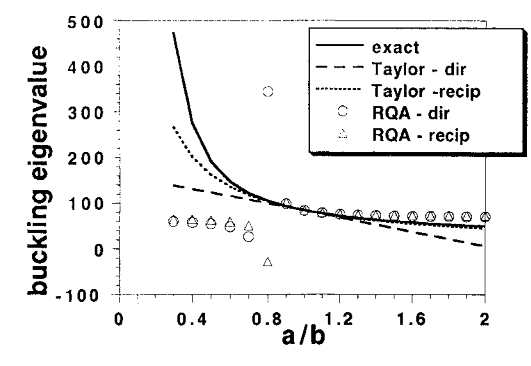

Fig. 7 Taylor series and Rayleigh quotient approximations for critical buckling loads of triangular panels of variable shape.

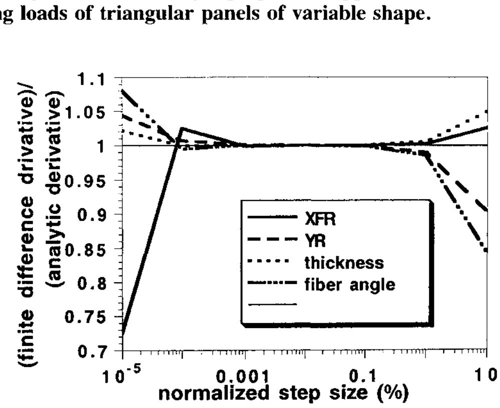

Fig. 8 Accuracy of finite difference derivatives of panel buckling eigenvalue with respect to sizing, fiber orientation, and shape design variables.

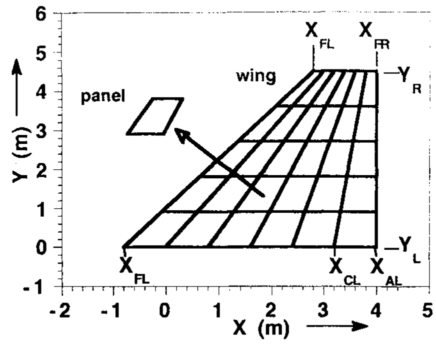

Fig. 9 Fighter-type wing, its spar and rib arrangement, and panel analyzed for buckling.

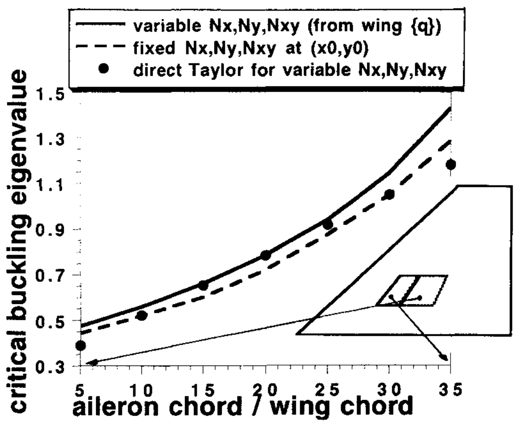

Fig. 10 Variation of critical panel buckling eigenvalue due to changes in wing spar locations.

order finite difference sensitivities can be obtained due to severe roundoff errors. This is not the case here, as Fig. 8 shows. This, and the fast convergence demonstrated, indicate that there are practically no ill-conditioning problems using simple polynomials in the present panel buckling analysis.

We next move to examine the integration of panel buckling analysis and sensitivity computations as presented here, with a wing box structural analysis based on the equivalent plate approach. As has already been discussed, the main appeal of the equivalent plate approach in wing structural analysis is in the simplicity of modeling and speed of computation, both extremely important for efficient multidisciplinary wing optimization. A fighter-type all-aluminum wing is shown in Fig. 9, together with the array of spars and ribs of its internal structure. A 3.5% parabolic airfoil is used. An airplane weight of 25,000 lb is assumed, and the wing is loaded in a uniform manner to support a 9-*g* pull-up maneuver (multiplied by 1.5 for safety factor). Skin thickness over the wing varies linearly from root to tip, $t(x, y) = 0.015\text{–}0.0026y$ (m). Shape variation of the internal structure is due to changes in the position of the rear spar, supporting a flaperon. As the flaperon chord to wing chord ratio varies, the design variable XCL (Fig. 9) changes. With the spars linked to each other to be equally spaced between XFL and XCL, all the spars move as a result of changes in XCL. We focus on one skin panel, shown in Fig. 9. Its change in shape and position, as the flaperon grows from 5 to 35%*c* is shown in Fig. 10.

The wing box analysis in this case is based on a 10-term Ritz polynomial satisfying cantilever boundary conditions at $y = 0$ (Ref. 23). Ten terms are also used in the Ritz series for the panel buckling analysis [Eq. (17)]. Analytic sensitivities of wing box response are discussed in Ref. 25. Analytic sensitivities of panel critical buckling eigenvalue were obtained by the technique described here.

In Fig. 10, critical buckling eigenvalues for the panel are shown as a function of global changes in the wing structure (flaperon chord size). The in-plane loads are obtained from stresses in the skin predicted by the wing analysis. When constant N_x, N_y, N_{xy} are used (based on their values at the center of the panel x_0, y_0), buckling eigenvalues are smaller compared with the case, in which N_x, N_y, and N_{xy} vary in a polynomial manner throughout the panel [as obtained from Eq. (45)]. The difference is smaller when the flaperon's chord is smaller. In that case, the panel is bigger and moves from the front to the center chord of the wing, thus carrying a larger in-plane load. An approximation based on direct Taylor series is shown in Fig. 10. No difficulties are encountered in the integration of wing analysis and sensitivity with panel buckling analysis and sensitivity computations, thus demonstrating the feasibility of combining two efficient modeling techniques for wing multidisciplinary design synthesis.

Conclusions

An efficient technique for computation of skin panel buckling constraints has been presented, tailored to the needs of multidisciplinary wing optimization. The formulation used, based on Ritz structural analysis using simple polynomials, makes it possible to obtain analytic sensitivities of buckling constraints with respect to shape, as well as sizing and fiber orientation design variables. No numerical integration is required. Closed-form expressions for stiffness and geometric stiffness matrix terms make it possible to identify dependence of those matrices on sizing, fiber angles, and shape design variables. Integration with equivalent plate wing structural analysis is natural, and the details have been described.

Numerical tests of the new capability, covering cases of rectangular, triangular, trapezoidal, and skew shapes with and without anisotropy, all demonstrate high accuracy and fast convergence. The fact that the derivation was done for simply supported boundary conditions presents no practical limitation, since edge rotational restraints with varying stiffnesses can be imposed through the addition of rotational springs along the boundary.[23] With the availability of analytic sensitivities, it becomes possible to assess the accuracy of finite difference sensitivities, and to construct Taylor series and Rayleigh quotient approximations. First-order Taylor series and Rayleigh quotient approximations based on direct and reciprocal variables were examined for the case of shape variation.

As the results presented here show, if some accuracy of analytic predictions can be sacrificed for the purpose of multidisciplinary preliminary design synthesis, then panel buckling analysis and sensitivities, using only 3–6 Ritz polynomial terms, can be obtained very efficiently. When integrated with wing structural analysis, aeroservoelastic analysis and aerodynamic loads and drag prediction,[23] the present buckling analysis capabilities add an important element to the integrated multidisciplinary design synthesis of actively controlled fiber composite wings.

Acknowledgments

The work reported here was supported by NASA. The help and encouragement of Hiro Miura, at NASA Ames Research Center, is gratefully acknowledged.

References

[1]Jones, R. M., *Mechanics of Composite Materials*, McGraw–Hill, New York, 1975.

[2]Whitney, J. M., *Structural Analysis of Laminated Anisotropic Plates*, Technomic, Lancaster, PA, 1987.

[3]Chamis, C. C., "Buckling of Anisotropic Composite Plates," *Proceedings of the American Society of Civil Engineers, Journal of the Structural Division*, Oct. 1969, pp. 2119–2139.

[4]Leissa, A. W., "Buckling of Laminated Plates and Shell Panels,"

Flight Dynamics Lab., Air Force Wright Aeronautical Labs., AFWAL-TR-85-3069, Wright-Patterson AFB, OH, June 1985.

[5]Nemeth, M. P., "Importance of Anisotropy on Buckling of Compression-Loaded Symmetric Composite Plates," *AIAA Journal*, Vol. 24, No. 11, 1986, pp. 1831–1835.

[6]Waddoups, M. E., McCullers, L. A., Olson, F. A., and Ashton, J. E., "Structural Synthesis of Anisotropic Panels," *Proceedings of the AIAA/ASME 11th Structures, Structural Dynamics, and Materials Conference* (Denver, CO), AIAA, New York, 1970.

[7]Schmit, L. A., and Farshi, B., "Optimum Design of Laminated Fibre Composite Plates," *International Journal for Numerical Methods in Engineering*, Vol. 11, 1977, pp. 623–640.

[8]Schmit, L. A., and Mehrinfar, M., "Multilevel Optimum Design of Structures with Fiber-Composite Stiffened-Panel Components," *AIAA Journal*, Vol. 20, No. 1, 1982, pp. 138–147.

[9]Schmit, L. A., and Ramanathan, R. K., "Multilevel Approach to Minimum Weight Design Including Buckling Constraints," *AIAA Journal*, Vol. 16, No. 2, 1978, pp. 97–104.

[10]Starnes, J. H., Jr., and Haftka, R. T., "Preliminary Design of Composite Wings for Buckling, Stress and Displacement Constraints," *Journal of Aircraft*, Vol. 16, 1979, pp. 564–570.

[11]McCullers, L. A., "Automated Design of Advanced Composite Structures," *Mechanics of Composite Materials*, edited by Z. Hashin, Pergamon, 1983, pp. 119–133.

[12]Hornung, G., Mathias, D. W., and Rohle, H., "Optimization of Wing Type Structures Including Stress and Buckling Constraints," Third Air Force/NASA Symposium on Recent Advances in Multidisciplinary Analysis and Optimization, San Francisco, CA, Sept. 1990.

[13]Haftka, R. T., and Gurdal, Z., *Elements of Structural Optimization*, 3rd ed., Kluwer, Dordrecht, The Netherlands, 1991, Chap. 11.

[14]Bicos, A. S., and Springer, G. S., "Design of a Composite Boxbeam," *Journal of Composite Materials*, Vol. 20, Jan. 1986.

[15]Lecina, G., and Petiau, C., "Advances in Optimal Design with Composite Materials," *Computer Aided Optimal Design: Structural and Mechanical Systems*, edited by C. A. Mota Soares, Springer–Verlag, Berlin, 1987, pp. 943–953.

[16]Ausman, J. D., Hangen, J. A., and Acevedo, D. A., "Application of a Local Panel Buckling Constraint Within Automated Multidisciplinary Structural Analysis and Design," AIAA Paper 92-1116, Feb. 1992.

[17]Ragon, S. A., Gurdal, Z., and Starnes, J. H., Jr., "Optimization of Composite Box-Beam Structures Including the Effects of Subcomponent Interaction," *Proceedings of the AIAA/ASME/ASCE/AHS/ASC 35th Structures, Structural Dynamics, and Materials Conference* (Hilton Head, SC), AIAA, Washington, DC, 1994, pp. 818–828 (AIAA Paper 94-1410).

[18]Smith, J., "General Plate Stability Using Higher Order Techniques," *Proceedings of the AIAA/ASME/ASCE/AHS/ASC 33rd Structures, Structural Dynamics, and Materials Conference* (Dallas, TX), AIAA, Washington, DC, 1992 (AIAA Paper 92-2283).

[19]Smith, J. P., "BUCKY—A *p* Finite Element Program for Plate Analysis," *Proceedings of the AIAA/ASME/ASCE/AHS/ASC 35th Structures, Structural Dynamics, and Materials Conference* (Hilton Head, SC), AIAA, Washington, DC, 1994, pp. 694–702 (AIAA Paper 94-1391).

[20]Jaunky, N., Knight, N. F., Jr., and Ambur, D. R., "Buckling of Arbitrary Quadrilateral Anisotropic Plates," *Proceedings of the AIAA/ASME/ASCE/AHS/ASC 35th Structures, Structural Dynamics, and Materials Conference* (Hilton Head, SC), AIAA, Washington, DC, 1994, pp. 493–503 (AIAA Paper 94-1369).

[21]Giles, G. L., "Equivalent Plate Analysis of Aircraft Wing Box Structures with General Planform Geometry," *Journal of Aircraft*, Vol. 23, No. 11, 1986, pp. 859–864.

[22]Giles, G. L., "Further Generalization of an Equivalent Plate Representation for Aircraft Structural Analysis," *Journal of Aircraft*, Vol. 26, No. 1, 1989, pp. 67–74.

[23]Livne, E., "Integrated Multidisciplinary Optimization of Actively Controlled Fiber Composite Wings," Ph.D. Dissertation, Mechanical, Aerospace and Nuclear Engineering Dept., Univ. of California, Los Angeles, CA, 1990.

[24]Singhvi, S., and Kapania, R. K., "Analytical Shape Sensitivities and Approximations of Modal Response of Generally Laminated Tapered Skew Plates," *Proceedings of the AIAA/ASME/ASCE/AHS/ASC 33rd Structures, Structural Dynamics, and Materials Conference* (Dallas, TX), AIAA, Washington, DC, 1992 (AIAA Paper 92-2391).

[25]Livne, E., "Analytical Sensitivities for Shape Optimization in Equivalent Plate Structural Wing Models," *Journal of Aircraft*, Vol. 31, No. 4, 1994, pp. 961–969.

[26]Livne, E., Sels, R., and Bhatia, K., "Lessons from Application of Equivalent Plate Structural Modeling to the HSCT Wing," *Journal of Aircraft*, Vol. 31, No. 4, 1994, pp. 953–960.

[27]Livne, E., "Equivalent Plate Structural Modeling for Wing Shape Optimization Including Transverse Shear," *AIAA Journal*, Vol. 32, No. 6, 1994, pp. 1278–1288.

[28]Fletcher, C. A. J., *Computational Galerkin Methods*, Springer–Verlag, New York, 1984.

[29]Leissa, A., and Jacob, K. I., "Three Dimensional Vibrations of Twisted Cantilevered Parallelepipeds," *Journal of Applied Mechanics*, Vol. 53, Sept. 1986, pp. 614–618.

[30]McGee, O. G., and Leissa, A. W., "Three Dimensional Free Vibrations of Thick Skewed Cantilevered Plates," *Journal of Sound and Vibration*, Vol. 144, No. 2, 1991, pp. 305–322.

[31]Koch, R. M., "Three Dimensional Vibrations of Doubly-Skewed, Helicoidal, Cantilevered Thick Shells," *Proceedings of the AIAA/ASME/ASCE/AHS/ASC 35th Structures, Structural Dynamics, and Materials Conference* (Hilton Head, SC), AIAA, Washington, DC, 1994, pp. 818–828 (AIAA Paper 94-1641).

[32]Tsai, S. W., and Hahn, H. T., *Introduction to Composite Materials*, Technomic, Westport, CT, 1980, p. 204.

[33]Bruhn, E. F., *Analysis and Design of Flight Vehicle Structures*, Tri State Offset Co., 1973, Chap. C5.

[34]Antona, E., and Romeo, G., "Analytical and Experimental Investigation on Advanced Composite Wing Box Structures in Bending Including Effects of Initial Imperfections and Crushing Pressure," *15th Congress of the International Council of the Aeronautical Sciences*, ICAS-86-4.2.3, London, Sept. 1986, pp. 255–261.

[35]Harvey, M., "Automated Finite Element Modeling of Wing Structures for Shape Optimization," M.S. Thesis, Dept. of Aeronautics and Astronautics, Univ. of Washington, Seattle, WA, 1993.

[36]Milosavljevic, R., "Buckling Analysis and Analytic Shape Sensitivities for Trapezoidal Panels in Wing Preliminary Design," M.S. Thesis, Dept. of Aeronautics and Astronautics, Univ. of Washington, Seattle, WA, July 1994.

[37]Haftka, R. T., and Gurdal, Z., *Elements of Structural Optimization*, 3rd ed., Kluwer, Dordrecht, The Netherlands, 1991, Chap. 6.

[38]Canfield, R. A., "High Quality Approximation of Eigenvalues in Structural Optimization," *AIAA Journal*, Vol. 28, No. 6, 1990, pp. 1116–1122.

[39]Canfield, R. A., "Design of Frames Against Buckling Using a Rayleigh Quotient Approximation," *AIAA Journal*, Vol. 31, No. 6, 1993, pp. 1143–1149.

[40]Kennedy, J. B., and Prabhakara, M. K., "Combined-Load Buckling of Orthotropic Skew Plates," *Journal of the Engineering Mechanics Division, ASCE*, Vol. 105, No. EMI, 1979, pp. 71–79.

[41]Timoshenko, S. P., and Gere, J. M., *Theory of Elastic Stability*, McGraw–Hill, New York, 1961, p. 393.

[42]Livne, E., and Li, W.-L., "Aeroservoelastic Aspects of Wing/Control Surface Planform Shape Optimization," *AIAA Journal*, Vol. 33, No. 2, 1995, pp. 302–311.